

Federated Learning Enables Big Data for Rare Cancer Boundary Detection

Sarthak Pati^{1,2,3,4,*}, Ujjwal Baid^{1,2,3,*}, Brandon Edwards^{5,*}, Micah Sheller⁵, Shih-Han Wang⁵, G Anthony Reina⁵, Patrick Foley⁵, Alexey Gruzdev⁵, Deepthi Karkada⁵, Christos Davatzikos^{1,2}, Chiharu Sako^{1,2}, Satyam Ghodasara², Michel Bilello^{1,2}, Suyash Mohan^{1,2}, Philipp Vollmuth⁷, Gianluca Brugnara⁷, Chandrakanth J Preetha⁷, Felix Sahm^{8,9}, Klaus Maier-Hein^{10,143}, Maximilian Zenk¹⁰, Martin Bendszus⁷, Wolfgang Wick^{8,11}, Evan Calabrese¹², Jeffrey Rudie¹², Javier Villanueva-Meyer¹², Soonmee Cha¹², Madhura Ingalthalikar¹³, Manali Jadhav¹³, Umang Pandey¹³, Jitender Saini¹⁴, John Garrett^{15,16}, Matthew Larson¹⁵, Robert Jeraj^{15,16}, Stuart Currie¹⁸, Russell Froom¹⁸, Kavi Fatania¹⁸, Raymond Y Huang¹⁹, Ken Chang²⁰, Carmen Balaña Quintero²¹, Jaume Capellades²², Josep Puig²³, Johannes Trenkler²⁴, Josef Pichler²⁵, Georg Necker²⁴, Andreas Haunschild²⁴, Stephan Meckel^{24,147}, Gaurav Shukla^{1,26}, Spencer Liem²⁷, Gregory S Alexander²⁸, Joseph Lombardo^{27,29}, Joshua D Palmer³⁰, Adam E Flanders³¹, Adam P Dicker²⁹, Haris I Sair^{32,33}, Craig K Jones³³, Archana Venkataraman³⁴, Meirui Jiang³⁵, Tiffany Y So³⁵, Cheng Chen³⁵, Pheng Ann Heng³⁵, Qi Dou³⁵, Michal Kozubek³⁶, Filip Lux³⁶, Jan Michálek³⁶, Petr Matula³⁶, Miloš Keřkovský³⁷, Tereza Kopřivová³⁷, Marek Dostál^{37,38}, Václav Vybihal³⁹, Michael A Vogelbaum⁴⁰, J Ross Mitchell^{87,88}, Joaquim Farinhas⁴², Joseph A Maldjian⁴³, Chandan Ganesh Bangalore Yogananda⁴³, Marco C Pinho⁴³, Divya Reddy⁴³, James Holcomb⁴³, Benjamin C Wagner⁴³, Benjamin M Ellingson^{44,45}, Timothy F Cloughesy⁴⁵, Catalina Raymond⁴⁴, Talia Oughourlian^{44,46}, Akifumi Hagiwara⁴⁶, Chencai Wang⁴⁶, Minh-Son To^{47,48}, Sargam Bhardwaj⁴⁷, Chee Chong⁵⁰, Marc Agzarian^{49,50}, Alexandre Xavier Falcão⁵¹, Samuel B Martins⁵², Bernardo C A Teixeira^{53,54}, Flávia Sprenger⁵⁴, David Menotti⁵⁵, Diego R Lucio⁵⁵, Pamela LaMontagne⁵⁶, Daniel Marcus⁵⁶, Benedikt Wiestler^{57,58}, Florian Kofler^{57,58,59}, Ivan Ezhov^{4,58,59}, Marie Metz⁵⁷, Rajan Jain^{60,61}, Matthew Lee⁶⁰, Yvonne W Lui⁶⁰, Richard McKinley⁶², Johannes Slotboom⁶², Piotr Radojewski⁶², Raphael Meier⁶², Roland Wiest⁶², Derrick Murcia⁶³, Eric Fu⁶³, Rourke Haas⁶³, John Thompson⁶³, David Ryan Ormond⁶³, Chaitra Badve⁶⁴, Andrew E Sloan^{65,66,67}, Vachan Vadmal⁶⁷, Kristin Waite⁶⁸, Rivka R Colen^{69,125}, Linmin Pei⁷⁰, Murat Ak⁶⁹, Ashok Srinivasan⁷¹, J Rajiv Bapuraj⁷¹, Arvind Rao⁷², Nicholas Wang⁷², Ota Yoshiaki⁷¹, Toshio Moritani⁷¹, Sevcen Turk⁷¹, Joonsang Lee⁷², Snehal Prabhudesai⁷², Fanny Morón⁷³, Jacob Mandel⁴⁹, Konstantinos Kamnitsas^{74,75}, Ben Glocker⁷⁴, Luke V M Dixon⁷⁶, Matthew Williams⁷⁷, Peter Zampakis⁷⁸, Vasileios Panagiotopoulos⁷⁹, Panagiotis Tsiganos⁸⁰, Sotiris Alexiou⁸¹, Ilias Haliassos⁸², Evangelia I Zacharaki⁸¹, Konstantinos Moustakas⁸¹, Christina Kalogeropoulou⁷⁸, Dimitrios M Kardamakis¹⁵⁰, Yoon Seong Choi⁸³, Seung-Koo Lee⁸³, Jong Hee Chang⁸³, Sung Soo Ahn⁸³, Bing Luo⁸⁴, Laila Poisson⁸⁵, Ning Wen^{84,148}, Pallavi Tiwari⁸⁶, Ruchika Verma^{86,88}, Rohan Bareja⁸⁶, Ipsa Yadav⁸⁶, Jonathan Chen⁸⁶, Neeraj Kumar^{87,88}, Marion Smits⁸⁹, Sebastian R van der Voort⁸⁹, Ahmed Alafandi⁸⁹, Fatih Incekara^{89,90}, Maarten MJ Wijnenga⁹¹, Georgios Kapsas⁸⁹, Renske Gahrman⁸⁹, Joost W Schouten⁹⁰, Hendrikus J Dubbink⁹³, Arnaud JPE Vincent⁹⁰, Martin J van den Bent⁹¹, Pim J French⁹¹, Stefan Klein⁹⁴, Yading Yuan⁹⁵, Sonam Sharma⁹⁵, Tzu-Chi Tseng⁹⁵, Saba Adabi⁹⁵, Simone P Niclou⁹⁶, Olivier Keunen⁹⁷, Ann-Christin Hau^{96,98}, Martin Vallières^{99,145}, David Fortin^{100,145}, Martin Lepage^{101,145}, Bennett Landman¹⁰², Karthik Ramadas¹⁰², Kaiwen Xu¹⁰³, Silky Chotali¹⁰⁴, Lola B Chambless¹⁰⁴, Akshitkumar Mistry¹⁰⁴, Reid C Thompson¹⁰⁴, Yuriy Gusev¹⁰⁵, Krithika Bhuvaneshwar¹⁰⁵, Anousheh Sayah¹⁰⁶, Camelia Bencheqroun¹⁰⁵, Anas Belouali¹⁰⁵, Subha Madhavan¹⁰⁵, Thomas C Booth^{107,108}, Alysha Chelliah¹⁰⁷, Marc Modat¹⁰⁷, Haris Shuaib^{109,110}, Carmen Dragos¹⁰⁹, Aly Abayazeed¹¹¹, Kenneth Kolodziej¹¹¹, Michael Hill¹¹¹, Ahmed Abbassy¹¹², Shady Gamal¹¹², Mahmoud Mekhaimar¹¹², Mohamed Qayati¹¹², Mauricio Reyes¹¹³, Ji Eun Park¹¹⁴, Jihye Yun¹¹⁴, Ho Sung Kim¹¹⁴, Abhishek Mahajan¹¹⁵, Mark Muzi¹¹⁶, Sean Benson¹¹⁷, Regina G H Beets-Tan^{152,153}, Jonas Teuwen¹¹⁷, Alejandro Herrera-Trujillo^{118,119}, Maria Trujillo¹¹⁹, William Escobar^{118,119}, Ana Abello¹¹⁹, Jose Berna^{119,120}, Jhon Gómez¹¹⁹, Joseph Choi¹²¹, Stephen Baek¹²², Yusung Kim¹²³, Heba Ismael¹²³, Bryan Allen¹²³, John M Buatti¹²³, Aikaterini Kotrotsou¹²⁶, Hongwei Li⁶, Tobias Weiss⁴¹, Michael Weller⁴¹, Andrea Bink¹⁷, Bertrand Pouymayou¹⁷, Hassan F Shaykh¹²⁷, Joel Saltz¹²⁸, Prateek Prasanna¹²⁸, Sampurna Shrestha¹²⁸, Kartik M Mani^{128,141}, David Payne¹⁴², Tahsin Kurc^{128,129}, Enrique Pelaez¹³⁰, Heydy Franco-Maldonado¹⁴⁴, Francis Loayza¹³⁰, Sebastian Quevedo¹³¹, Pamela Guevara¹³², Esteban Torche¹³², Cristobal Mendoza¹³², Franco Vera¹³², Elvis Ríos¹³², Eduardo López¹³², Sergio A Velastin¹³³, Godwin Ogbale¹³⁴, Dotun Oyekunle¹³⁴, Olubunmi Odafe-Oyibotha¹³⁵, Babatunde Osobu¹³⁴, Mustapha Shu'aibu¹³⁶, Adeleye Dorcas¹³⁷, Mayowa Soneye¹³⁴, Farouk Dako^{2,124}, Amber L Simpson^{110,138}, Mohammad Hamghalam^{138,149}, Jacob J Peoples¹³⁸, Ricky Hu¹³⁸, Anh Tran¹³⁸, Danielle Cutler¹⁴⁶, Fabio Y Moraes¹⁵¹, Michael A Boss¹³⁹, James Gimpel¹³⁹, Deepak Kattil Veetil¹³⁹,

Kendall Schmidt^{92, 93}, Brian Bialecki⁹², Sailaja Marella¹³⁹, Cynthia Price¹³⁹, Lisa Cimino¹³⁹, Charles Appgar¹³⁹, Prashant Shah^{5, 94}, Bjoern Menze^{4, 6, 95}, Jill S Barnholtz-Sloan^{68, 140, 96}, Jason Martin⁵, and Spyridon Bakas^{1, 2, 3, 5, 97}

- ¹ Center for Biomedical Image Computing and Analytics (CBICA), University of Pennsylvania, Philadelphia, Pennsylvania, USA.
- ² Department of Radiology, Perelman School of Medicine, University of Pennsylvania, Philadelphia, Pennsylvania, USA.
- ³ Department of Pathology and Laboratory Medicine, Perelman School of Medicine, University of Pennsylvania, Philadelphia, Pennsylvania, USA.
- ⁴ Department of Informatics, Technical University of Munich, Munich, Bavaria, Germany.
- ⁵ Intel Corporation, Santa Clara, California, USA.
- ⁶ Department of Quantitative Biomedicine, University of Zurich, Zurich, Switzerland.
- ⁷ Department of Neuroradiology, Heidelberg University Hospital, Heidelberg, Germany.
- ⁸ Clinical Cooperation Unit Neuropathology, German Cancer Consortium (DKTK) within the German Cancer Research Center (DKFZ), Heidelberg, Germany.
- ⁹ Department of Neuropathology, Heidelberg University Hospital, Heidelberg, Germany.
- ¹⁰ Division of Medical Image Computing, German Cancer Research Center, Heidelberg, Germany.
- ¹¹ Neurology Clinic, Heidelberg University Hospital, Heidelberg, Germany.
- ¹² Department of Radiology & Biomedical Imaging, University of California San Francisco, San Francisco, California, USA.
- ¹³ Symbiosis Center for Medical Image Analysis, Symbiosis International University, Pune, Maharashtra, India.
- ¹⁴ Department of Neuroimaging and Interventional Radiology, National Institute of Mental Health and Neurosciences, Bangalore, Karnataka, India.
- ¹⁵ Department of Radiology, School of Medicine and Public Health, University of Wisconsin, Madison, Wisconsin, USA.
- ¹⁶ Department of Medical Physics, School of Medicine and Public Health, University of Wisconsin, Madison, Wisconsin, USA.
- ¹⁷ Department of Neuroradiology, Clinical Neuroscience Center, University Hospital Zurich and University of Zurich, Zurich, Switzerland.
- ¹⁸ Leeds Teaching Hospitals Trust, Department of Radiology, Leeds, United Kingdom.
- ¹⁹ Department of Radiology, Brigham and Women's Hospital, Harvard Medical School, Boston, Massachusetts, USA.
- ²⁰ Athinoula A. Martinos Center for Biomedical Imaging, Massachusetts General Hospital, Charlestown, Massachusetts, USA.
- ²¹ Catalan Institute of Oncology, Badalona, Spain.
- ²² Consorci MAR Parc de Salut de Barcelona, Catalonia, Spain.
- ²³ Department of Radiology (IDI), Girona Biomedical Research Institute (IdIBGi), Josep Trueta University Hospital, Girona, Spain.
- ²⁴ Institute of Neuroradiology, Neuromed Campus (NMC), Kepler University Hospital Linz, Linz, Austria.
- ²⁵ Department of Neurooncology, Neuromed Campus (NMC), Kepler University Hospital Linz, Linz, Austria.
- ²⁶ Department of Radiation Oncology, Christiana Care Health System, Philadelphia, Pennsylvania, USA.
- ²⁷ Sidney Kimmel Medical College, Thomas Jefferson University, Philadelphia, Pennsylvania, USA.
- ²⁸ Department of Radiation Oncology, University of Maryland, Baltimore, Maryland, USA.
- ²⁹ Department of Radiation Oncology, Sidney Kimmel Cancer Center, Thomas Jefferson University, Philadelphia, Pennsylvania, USA.
- ³⁰ Department of Radiation Oncology, The James Cancer Hospital and Solove Research Institute, The Ohio State University Comprehensive Cancer Center, Columbus, Ohio, USA.
- ³¹ Department of Radiology, Sidney Kimmel Cancer Center, Thomas Jefferson University, Philadelphia, Pennsylvania, USA.
- ³² The Russell H. Morgan Department of Radiology and Radiological Science, Johns Hopkins University School of Medicine, Baltimore, Maryland, USA.
- ³³ The Malone Center for Engineering in Healthcare, The Whiting School of Engineering, Johns Hopkins University, Baltimore, Maryland, USA.
- ³⁴ Department of Electrical and Computer Engineering, Whiting School of Engineering, Johns Hopkins University, Baltimore, Maryland, USA.
- ³⁵ The Chinese University of Hong Kong, Hong Kong, China.
- ³⁶ Centre for Biomedical Image Analysis, Faculty of Informatics, Masaryk University, Brno, Czech Republic.
- ³⁷ Department of Radiology and Nuclear Medicine, Faculty of Medicine, Masaryk University, Brno and University Hospital Brno, Czech Republic.
- ³⁸ Department of Biophysics, Faculty of Medicine, Masaryk University, Brno, Czech Republic.
- ³⁹ Department of Neurosurgery, Faculty of Medicine, Masaryk University, Brno, and University Hospital and Czech Republic.
- ⁴⁰ Department of Neuro Oncology, H. Lee Moffitt Cancer Center and Research Institute, Tampa, Florida, USA.
- ⁴¹ Department of Neurology, Clinical Neuroscience Center, University Hospital Zurich and University of Zurich, Zurich, Switzerland.
- ⁴² Department of Radiology, H. Lee Moffitt Cancer Center and Research Institute, Tampa, Florida, USA.
- ⁴³ University of Texas Southwestern Medical Center, Dallas, Texas, USA.
- ⁴⁴ UCLA Brain Tumor Imaging Laboratory (BTIL), Center for Computer Vision and Imaging Biomarkers, Department of Radiological Sciences, David Geffen School of Medicine, University of California Los Angeles, Los Angeles, California, USA.
- ⁴⁵ UCLA Neuro-Oncology Program, Department of Neurology, David Geffen School of Medicine, University of California Los Angeles, Los Angeles, California, USA.
- ⁴⁶ Department of Radiological Sciences, David Geffen School of Medicine, University of California Los Angeles, Los Angeles, California, USA.
- ⁴⁷ College of Medicine and Public Health, Flinders University, Bedford Park, South Australia, Australia.
- ⁴⁸ Division of Surgery and Perioperative Medicine, Flinders Medical Centre, Bedford Park, South Australia, Australia.
- ⁴⁹ Department of Neurology, Baylor College of Medicine, Houston, Texas, USA.

- ⁵⁰ South Australia Medical Imaging, Flinders Medical Centre, Bedford Park, South Australia.
- ⁵¹ Institute of Computing, University of Campinas, Campinas, São Paulo, Brazil.
- ⁵² Federal Institute of São Paulo, Campinas, São Paulo, Brazil.
- ⁵³ Instituto de Neurologia de Curitiba, Curitiba, Paraná, Brazil.
- ⁵⁴ Department of Radiology, Hospital de Clínicas da Universidade Federal do Paraná, Curitiba, Paraná, Brazil.
- ⁵⁵ Department of Informatics, Universidade Federal do Paraná, Curitiba, Paraná, Brazil.
- ⁵⁶ Department of Radiology, Washington University in St. Louis, St. Louis, Missouri, USA.
- ⁵⁷ Department of Diagnostic and Interventional Neuroradiology, School of Medicine, Klinikum rechts der Isar, Technical University of Munich, Germany.
- ⁵⁸ TranslaTUM (Zentralinstitut für translationale Krebsforschung der Technischen Universität München), Klinikum rechts der Isar, Munich, Germany.
- ⁵⁹ Image-Based Biomedical Modeling, Department of Informatics, Technical University of Munich, Munich, Germany.
- ⁶⁰ Department of Radiology, NYU Grossman School of Medicine, New York, New York, USA.
- ⁶¹ Department of Neurosurgery, NYU Grossman School of Medicine, New York, New York, USA.
- ⁶² Support Center for Advanced Neuroimaging, University Institute of Diagnostic and Interventional Neuroradiology, University Hospital Bern, Inselspital, University of Bern, Bern, Switzerland.
- ⁶³ Department of Neurosurgery, Anschutz Medical Campus, University of Colorado, Aurora, Colorado, USA.
- ⁶⁴ Department of Radiology, University Hospitals Cleveland, Cleveland, Ohio, USA.
- ⁶⁵ Department of Neurological Surgery, University Hospitals-Seidman Cancer Center, Cleveland, Ohio, USA.
- ⁶⁶ Case Comprehensive Cancer Center, Cleveland, Ohio, USA.
- ⁶⁷ Department of Neurosurgery, Case Western Reserve University School of Medicine, Cleveland, Ohio, USA.
- ⁶⁸ National Cancer Institute, National Institute of Health, Division of Cancer Epidemiology and Genetics, Bethesda, Maryland, USA.
- ⁶⁹ Department of Radiology, Neuroradiology Division, University of Pittsburgh, Pittsburgh, Pennsylvania, USA.
- ⁷⁰ University of Pittsburgh Medical Center, Pittsburgh, Pennsylvania, USA.
- ⁷¹ Department of Neuroradiology, University of Michigan, Ann Arbor, Michigan, USA.
- ⁷² Department of Computational Medicine and Bioinformatics, University of Michigan, Ann Arbor, Michigan, USA.
- ⁷³ Department of Radiology, Baylor College of Medicine, Houston, Texas, USA.
- ⁷⁴ Department of Computing, Imperial College London, London, United Kingdom.
- ⁷⁵ Institute of Biomedical Engineering, Department of Engineering Science, University of Oxford, Oxford, United Kingdom.
- ⁷⁶ Department of Radiology, Imperial College NHS Healthcare Trust, London, United Kingdom.
- ⁷⁷ Computational Oncology Group, Institute for Global Health Innovation, Imperial College London, London, United Kingdom.
- ⁷⁸ Department of NeuroRadiology, University of Patras, Patras, Greece.
- ⁷⁹ Department of Neurosurgery, University of Patras, Patras, Greece.
- ⁸⁰ Clinical Radiology Laboratory, Department of Medicine, University of Patras, Patras, Greece.
- ⁸¹ Department of Electrical and Computer Engineering, University of Patras, Patras, Greece.
- ⁸² Department of Neuro-Oncology, University of Patras, Patras, Greece.
- ⁸³ Yonsei University College of Medicine, Seoul, Korea.
- ⁸⁴ Department of Radiation Oncology, Henry Ford Health System, Detroit, Michigan, USA.
- ⁸⁵ Public Health Sciences, Henry Ford Health System, Detroit, Michigan, USA.
- ⁸⁶ Case Western Reserve University, Cleveland, Ohio, USA.
- ⁸⁷ University of Alberta, Edmonton, Alberta, Canada.
- ⁸⁸ Alberta Machine Intelligence Institute, Edmonton, Alberta, Canada.
- ⁸⁹ Department of Radiology and Nuclear Medicine, Erasmus MC University Medical Centre Rotterdam, Rotterdam, Netherlands.
- ⁹⁰ Department of Neurosurgery, Brain Tumor Center, Erasmus MC University Medical Centre Rotterdam, Rotterdam, Netherlands.
- ⁹¹ Department of Neurology, Brain Tumor Center, Erasmus MC Cancer Institute, Rotterdam, Netherlands.
- ⁹² Data Science Institute, American College of Radiology, Reston, VA, USA.
- ⁹³ Department of Pathology, Brain Tumor Center, Erasmus MC Cancer Institute, Rotterdam, Netherlands.
- ⁹⁴ Biomedical Imaging Group Rotterdam, Department of Radiology and Nuclear Medicine, Erasmus MC University Medical Centre Rotterdam, Rotterdam, Netherlands.
- ⁹⁵ Department of Radiation Oncology, Icahn School of Medicine at Mount Sinai, New York, New York, USA.
- ⁹⁶ NORLUX Neuro-Oncology Laboratory, Department of Cancer Research, Luxembourg Institute of Health, Luxembourg, Luxembourg.
- ⁹⁷ Translation Radiomics, Department of Cancer Research, Luxembourg Institute of Health, Luxembourg.
- ⁹⁸ Luxembourg Center of Neuropathology, Laboratoire National De Santé, Luxembourg.
- ⁹⁹ Department of Computer Science, Université de Sherbrooke, Sherbrooke, Quebec, Canada.
- ¹⁰⁰ Division of Neurosurgery and Neuro-Oncology, Faculty of Medicine and Health Science, Université de Sherbrooke, Sherbrooke, Quebec, Canada.
- ¹⁰¹ Department of Nuclear Medicine and Radiobiology, Sherbrooke Molecular Imaging Centre, Université de Sherbrooke, Sherbrooke, Quebec, Canada.
- ¹⁰² Electrical and Computer Engineering, Vanderbilt University, Nashville, Tennessee, USA.
- ¹⁰³ Department of Computer Science, Vanderbilt University, Nashville, Tennessee, USA.
- ¹⁰⁴ Department of Neurosurgery, Vanderbilt University Medical Center, Nashville, Tennessee, USA.
- ¹⁰⁵ Innovation Center for Biomedical Informatics (ICBI), Georgetown University, Washington, District of Columbia, USA.
- ¹⁰⁶ Division of Neuroradiology & Neurointerventional Radiology, MedStar Georgetown University Hospital, Department of Radiology, Washington, DC, USA.

- ¹⁰⁷ School of Biomedical Engineering & Imaging Sciences, King's College London, London, United Kingdom.
- ¹⁰⁸ Department of Neuroradiology, Ruskin Wing, King's College Hospital NHS Foundation Trust, London, United Kingdom.
- ¹⁰⁹ Stoke Mandeville Hospital, Mandeville Road, Aylesbury, United Kingdom.
- ¹¹⁰ Department of Biomedical and Molecular Sciences, Queen's University, Kingston, ON, Canada.
- ¹¹¹ Neosoma Inc., Groton, Massachusetts, USA.
- ¹¹² University of Cairo School of Medicine, Giza, Egypt.
- ¹¹³ University of Bern, Switzerland.
- ¹¹⁴ Department of Radiology, Asan Medical Center, Seoul, South Korea.
- ¹¹⁵ The Clatterbridge Cancer Centre NHS Foundation Trust Pembroke Place, Liverpool, United Kingdom
- ¹¹⁶ Department of Radiology, University of Washington, Seattle, Washington, USA.
- ¹¹⁷ Netherlands Cancer Institute, Amsterdam, Netherlands.
- ¹¹⁸ Clínica Imbanaco Grupo Quirón Salud, Cali, Colombia.
- ¹¹⁹ Universidad del Valle, Cali, Colombia.
- ¹²⁰ The University of Edinburgh, Edinburgh, United Kingdom.
- ¹²¹ Department of Industrial and Systems Engineering, University of Iowa, Iowa, USA.
- ¹²² Department of Industrial and Systems Engineering, Department of Radiation Oncology, University of Iowa, Iowa, USA.
- ¹²³ Department of Radiation Oncology, University of Iowa, Iowa, USA.
- ¹²⁴ Center for Global Health, Perelman School of Medicine, University of Pennsylvania, Philadelphia, Pennsylvania, USA.
- ¹²⁵ Department of Diagnostic Radiology, University of Texas MD Anderson Cancer Center, Houston, Texas, USA.
- ¹²⁶ MD Anderson Cancer Center, University of Texas, Houston, Texas, USA.
- ¹²⁷ University of Alabama in Birmingham, Birmingham, Alabama, USA.
- ¹²⁸ Department of Biomedical Informatics, Stony Brook University, Stony Brook, New York, USA.
- ¹²⁹ Scientific Data Group, Oak Ridge National Laboratory, Oak Ridge, Tennessee, USA.
- ¹³⁰ Escuela Superior Politécnica del Litoral, Guayaquil, Guayas, Ecuador.
- ¹³¹ Universidad Católica de Cuenca, Cuenca, Ecuador.
- ¹³² Universidad de Concepción, Concepción, Biobío, Chile.
- ¹³³ School of Electronic Engineering and Computer Science, Queen Mary University of London, London, United Kingdom.
- ¹³⁴ Department of Radiology, University College Hospital Ibadan, Oyo, Nigeria.
- ¹³⁵ Clinix Healthcare, Lagos, Lagos, Nigeria.
- ¹³⁶ Department of Radiology, Muhammad Abdullahi Wase Teaching Hospital, Kano, Nigeria.
- ¹³⁷ Department of Radiology, Obafemi Awolowo University Ile-Ife, Ile-Ife, Osun, Nigeria.
- ¹³⁸ School of Computing, Queen's University, Kingston, Ontario, Canada.
- ¹³⁹ Center for Research and Innovation, American College of Radiology, Philadelphia, Pennsylvania, USA.
- ¹⁴⁰ Center for Biomedical Informatics and Information Technology, National Cancer Institute (NCI), National Institute of Health, Bethesda, Maryland, USA.
- ¹⁴¹ Department of Radiation Oncology, Stony Brook University, Stony Brook, New York, USA.
- ¹⁴² Department of Radiology, Stony Brook University, Stony Brook, New York, USA.
- ¹⁴³ Pattern Analysis and Learning Group, Department of Radiation Oncology, Heidelberg University Hospital, Heidelberg, Germany.
- ¹⁴⁴ Sociedad de Lucha Contral el Cancer - SOLCA, Guayaquil Ecuador.
- ¹⁴⁵ Centre de Recherche du Centre Hospitalière Universitaire de Sherbrooke, Sherbrooke, Quebec, Canada.
- ¹⁴⁶ The Faculty of Arts & Sciences, Queen's University, Kingston, Ontario, Canada.
- ¹⁴⁷ Institute of Diagnostic and Interventional Neuroradiology, RKH Klinikum Ludwigsburg, Ludwigsburg, Germany.
- ¹⁴⁸ SJTU-Ruijing-UIH Institute for Medical Imaging Technology, Ruijin Hospital, Shanghai Jiao Tong University School of Medicine, No. 197, Rui Jin 2nd Road, Shanghai 200025, China.
- ¹⁴⁹ Department of Electrical Engineering, Qazvin Branch, Islamic Azad University, Qazvin, Iran.
- ¹⁵⁰ Department of Radiation Oncology, University of Patras, Patras, Greece.
- ¹⁵¹ Department of Oncology, Queen's University, Kingston, Ontario, Canada.
- ¹⁵² Department of Radiology, Netherlands Cancer Institute, Amsterdam, Netherlands.
- ¹⁵³ GROW School of Oncology and Developmental Biology, Maastricht, Netherlands.

* These authors contributed equally to this work.

§ Corresponding author: {sbakas@upenn.edu}

Abstract. Although machine learning (ML) has shown promise in numerous domains, there are concerns about generalizability to out-of-sample data. This is currently addressed by centrally sharing ample, and importantly diverse, data from multiple sites. However, such centralization is challenging to scale (or even not feasible) due to various limitations. Federated ML (FL) provides an alternative to train accurate and generalizable ML models, by only sharing numerical model updates. Here we present findings from the largest FL study to-date, involving data from 71 healthcare institutions across 6 continents, to generate an automatic tumor boundary detector for the rare disease of glioblastoma, utilizing the largest dataset of such patients ever used in the literature (25,256 MRI scans from 6,314 patients). We demonstrate a 33% improvement over a publicly trained model to delineate the surgically targetable tumor, and 23% improvement over the tumor’s entire extent. We anticipate our study to: 1) enable more studies in healthcare informed by large and diverse data, ensuring meaningful results for rare diseases and underrepresented populations, 2) facilitate further quantitative analyses for glioblastoma via performance optimization of our consensus model for eventual public release, and 3) demonstrate the effectiveness of FL at such scale and task complexity as a paradigm shift for multi-site collaborations, alleviating the need for data sharing.

Keywords: federated learning, deep learning, convolutional neural network, segmentation, brain tumor, glioma, glioblastoma, FeTS, BraTS

Advances in machine learning (*ML*), and particularly deep learning (*DL*), have shown promise in addressing complex healthcare problems^{1–14}. However, there are concerns about generalizability on data from sources that did not participate in model training, i.e., “out-of-sample” data^{15,16}. Literature indicates that training robust and accurate models requires large amounts of data^{17–19}, the diversity of which affects model generalizability to “out-of-sample” cases²⁰. To address these concerns, models need to be trained on data originating from numerous sites representing diverse population samples. The current paradigm for such multi-site collaborations is “centralized learning” (*CL*), in which data from different sites are shared to a centralized location following inter-site agreements^{20–23}. However, such data centralization is difficult to scale (and might not even be feasible), especially at a global scale, due to concerns^{24,25} relating to privacy, data-ownership, intellectual property, technical challenges (e.g., network and storage limitations), as well as compliance with varying regulatory policies (e.g., Health Insurance Portability and Accountability Act (HIPAA) of the United States²⁶ and the General Data Protection Regulation (GDPR) of the European Union²⁷). In contrast to this centralized paradigm, “federated learning” (*FL*) describes an approach where models are trained by only sharing model parameter updates from decentralized data (i.e., each site retains its data locally)^{24,25,28–30}, without sacrificing performance when compared to CL-trained models^{25,29,31–35}. Thus, FL can offer an alternative to CL, potentially creating a paradigm shift that alleviates the need for data sharing, and hence increase access to geographically-distinct collaborators, thereby increasing the size and diversity of data used to train ML models.

FL has tremendous potential in healthcare^{36,37}, particularly towards addressing health disparities, under-served populations, and “rare” diseases³⁸, by enabling ML models to gain knowledge from ample and diverse data that would otherwise not be available. With that in mind, here we focus on the “rare” disease of glioblastoma, and particularly on the detection of its extent using multi-parametric magnetic resonance imaging (mpMRI) scans³⁹. While glioblastoma is the most common malignant primary brain tumor^{40–42}, it is still classified as a “rare” disease, as its incidence rate (i.e., 3/100,000 people) is substantially lower than

the rare disease definition rate (i.e., $< 10/100,000$ people)³⁸. This means that single sites cannot collect large and diverse datasets to train robust and generalizable ML models, and necessitates collaboration between geographically distinct sites. Despite extensive efforts to improve prognosis of glioblastoma patients with intense multimodal therapy, their median overall survival is only 14.6 months after standard-of-care treatment, and 4 months without treatment⁴³. Although the subtyping of glioblastoma has been improved⁴⁴ and the standard-of-care treatment options have expanded during the last twenty years, there have been no substantial improvements in overall survival⁴⁵. This reflects the major obstacle in treating these tumors that is their intrinsic heterogeneity^{40,42}, and the need for analyses of larger and more diverse data towards better understanding the disease. In terms of radiologic appearance, glioblastomas comprise 3 main sub-compartments, defined as i) the “enhancing tumor” (ET), representing the vascular blood-brain barrier breakdown within the tumor, ii) the “tumor core” (TC), which includes the ET and the necrotic (NCR) part, and represents the surgically relevant part of the tumor, and iii) the “whole tumor” (WT), which is defined by the union of the TC and the peritumoral edematous/infiltrated tissue (ED), and represents the complete tumor extent relevant to radiotherapy (Fig. 1.b). Detecting these sub-compartment boundaries therefore defines a multi-parametric multi-class learning problem^{46–50}, and is a critical first step towards further quantifying and assessing this heterogeneous rare disease and ultimately influencing clinical decision-making.

Co-authors in this study have previously introduced FL in healthcare in a simulated setting²⁹ and evaluated different FL approaches²⁵ for the same use case as the present study, i.e., detecting the boundaries of glioblastoma sub-compartments. Findings from these studies supported the superiority of the FL approach used in the present study (i.e., based on an aggregation server^{24,28}), which had almost identical performance to CL. The present study describes the largest to-date global FL effort to develop an accurate and generalizable ML model for detecting glioblastoma sub-compartment boundaries, based on 25,256 MRI scans (over 5TB) of 6,314 glioblastoma patients from 71 geographically distinct sites, across 6 continents (Fig. 1.a). Notably, this describes the largest and most diverse dataset of glioblastoma patients ever considered in the literature. It was the use of FL that successfully enabled our ML model to gain knowledge from such an unprecedented dataset. The extended global footprint and the task complexity is what sets this study apart from current literature, since it dealt with a multi-parametric multi-class problem with reference standards that require expert clinicians following an involved manual annotation protocol, rather than recording a categorical entry from medical records^{30,51}. Moreover, varying characteristics of the mpMRI data due to scanner hardware and acquisition protocol differences^{52,53} were handled at each collaborating site via established harmonized preprocessing pipelines^{54–57}.

The scientific contributions of this manuscript can be summarized by i) the insights garnered during this work that can pave the way for more successful FL studies of increased scale and task complexity, ii) making a potential impact for the treatment of the rare disease of glioblastoma, by eventually publicly releasing an optimized trained consensus model for use in resource-constrained clinical settings, and iii) demonstrating the effectiveness of FL at such scale and task complexity as a paradigm shift redefining multi-site collaborations, while alleviating the need for data sharing.

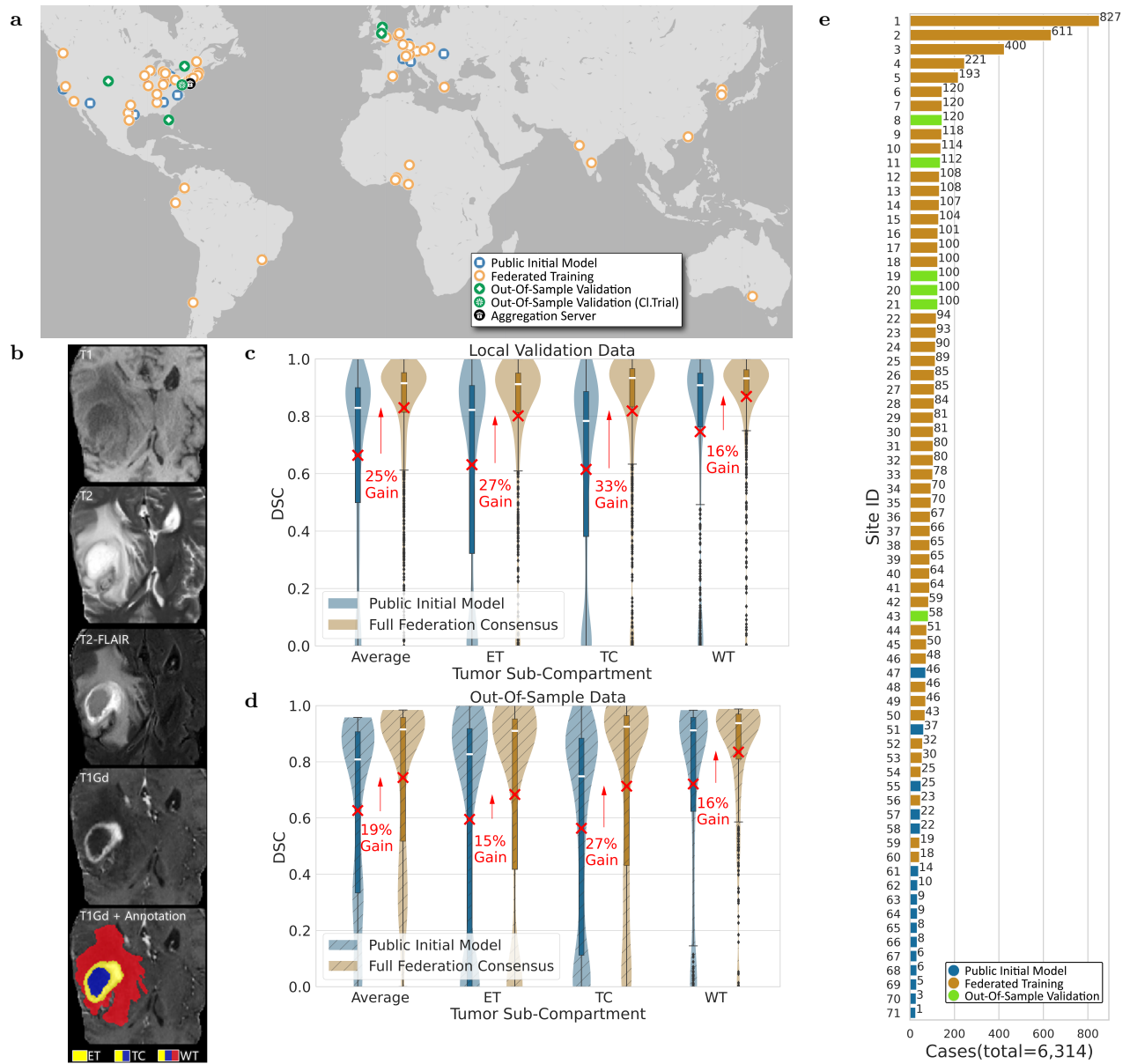


Fig. 1: Representation of the study's global scale, diversity, and complexity. **a**, The map of all sites involved in the development of FL consensus model. **b**, example of a glioblastoma mpMRI scan with corresponding reference annotations of the tumor sub-compartments. **c-d**, comparative performance evaluation of the final consensus model with the public initial model on the collaborators' local validation data (in **c**) and on the complete out-of-sample data (in **d**), per tumor sub-compartment. Note the box and whiskers inside each violin plot, represent the true min and max values. The top and bottom of each "box" depict the 3rd and 1st quartile of each measure. The white line and the red \times , within each box, indicate the median and mean values, respectively. The fact that these are not necessarily at the centre of each box indicates the skewness of the distribution over different cases. The "whiskers" drawn above and below each box depict the extremal observations still within 1.5 times the interquartile range, above the 3rd or below the 1st quartile. **e**, number of contributed cases per collaborating site.

Methods

Data

The data considered in this study described patient populations with adult-type diffuse glioma⁴⁴, and specifically displaying the radiological features of glioblastoma, scanned with mpMRI to characterize the anatomical tissue structure³⁹. Each case is specifically described by i) native T1-weighted (T1), ii) Gadolinium-enhanced T1-weighted (T1Gd), iii) T2-weighted (T2), and iv) T2-weighted-Fluid-Attenuated-Inversion-Recovery (T2-FLAIR) MRI scans. Cases with any of these sequences missing were not included in the study. Note that no inclusion/exclusion criterion applied relating to the type of acquisition (i.e., both 2D axial and 3D acquisitions were included, with a preference for 3D if available), or the exact type of sequence (e.g., MP-RAGE vs SPGR). The only exclusion criterion was for T1-FLAIR scans that were intentionally excluded to avoid mixing varying tissue appearance due to the type of sequence, across native T1-weighted scans.

The eligibility of collaborating sites to participate in the federation was determined based on data availability, and approval by their respective institutional review board. 55 sites participated as independent collaborators in the study defining a dataset of 6,083 cases. The MRI scanners used for data acquisition were from multiple vendors (i.e., Siemens, GE, Philips, Hitachi, Toshiba), with magnetic field strength ranging from 1T to 3T. The data from all 55 collaborating sites followed a male:female ratio of 1.47 : 1 with age ranging between 7 and 94 years.

From all 55 collaborating sites, 49 were chosen to be part of the training phase, and 6 sites were categorized as “out-of-sample”, i.e., none of these were part of the training stage. These specific 6 out-of-sample sites (Site IDs: 8, 11, 19, 20, 21, 43) were allocated based on their availability, i.e., they have indicated an expected delayed participation rendering them optimal for model generalizability validation. One of these 6 out-of-sample sites (Site 11) contributed aggregated *a priori* data from a multi-site randomized clinical trial for newly diagnosed glioblastoma (ClinicalTrials.gov Identifier: NCT00884741, RTOG0825^{58,59}, ACRIN6686^{60,61}), with inherent diversity benefiting the intended generalizability validation purpose. The American College of Radiology (ACR - Site 11) serves as the custodian of this trial’s imaging data on behalf of ECOG-ACRIN, who made the data available for this study. Following screening for availability of the 4 required mpMRI scans with sufficient signal-to-noise ratio judged by visual observation, a subset of 362 cases from the original trial data were included in this study. The out-of-sample data totaled 590 cases intentionally held-out of the federation, with the intention of validating the consensus model in completely unseen cases. To facilitate further such generalizability evaluation without burdening the collaborating sites, a subset consisting of 332 cases (including the multi-site clinical data provided by ACR) from this out-of-sample data was aggregated, to serve as the “*centralized out-of-sample*” dataset. Furthermore, the 49 sites participating in the training phase define a collective dataset of 5,493 cases. The exact 49 site IDs are: 1, 2, 3, 4, 5, 6, 7, 9, 10, 12, 13, 14, 15, 16, 17, 18, 22, 23, 24, 25, 26, 27, 28, 29, 30, 31, 32, 33, 34, 35, 36, 37, 38, 39, 40, 41, 42, 44, 45, 46, 48, 49, 50, 52, 53, 54, 56, 59, 60. These cases were automatically split at each site following a 4 : 1 ratio between cases for training and local validation. During the federated training phase the data used for the public initial model were also included as a dataset from a separate node, such that the contribution of sites providing the publicly available data is not forgotten within the global consensus model. This

results in the final consensus model being developed based on data from 71 sites over a total dataset of 6,314 cases.

Harmonized Data Preprocessing

Once each collaborating site identified their local data, they were asked to use the preprocessing functionality of the software platform we provided. This functionality follows the harmonized data preprocessing protocol defined by the BraTS challenge^{54–57}, to account for inter-site acquisition protocol variations, e.g., 3D vs 2D axial plane acquisitions.

The neural network architecture

The trained model to delineate the different tumor sub-compartments was based on the popular 3D U-Net with residual connections (3D-ResUNet)^{62–66}. The network had 30 base filters, with a learning rate of $lr = 5 \times 10^{-5}$ optimized using the Adam optimizer⁶⁷. For the loss function used in training, we used the generalized *DSC* score^{68,69} (represented mathematically in Eq. 1) on the absolute complement of each tumor sub-compartment independently. Such mirrored *DSC* loss has been shown to capture variations in smaller regions better⁷⁰. No penalties were used in the loss function, due to our use of ‘mirrored’ *DSC* loss^{71–73}. The final layer of the model was a sigmoid layer, providing three channel outputs for each voxel in the input volume, one output channel per tumor sub-compartment. While the generalized *DSC* score was calculated using a binarized version of the output (check sigmoid value against the threshold 0.5) for the final prediction, we used the floating point *DSC*⁷⁴ during the training process.

$$DSC = \frac{2 \|RL \odot PM\|_1}{\|RL\|_1 + \|PM\|_1} \quad (1)$$

where *RL* serves as the reference label, *PM* is the predicted mask, \odot is the Hadamard product⁷⁵ (i.e., component wise multiplication), and $\|x\|_1$ is the L1-norm⁷⁶, i.e., sum of the absolute values of all components).

The Federation

The collaborative network of the present study spans 6 continents (Fig. 1), with data from 71 geographically distinct sites. The training process was initiated when each collaborator securely connected to a central aggregation server, which resided behind a firewall at the University of Pennsylvania. As soon as the secure connection was established, the public initial model was passed to the collaborating site. Using FL based on an aggregation server, collaborating sites then trained the same network architecture on their local data for one epoch, and shared model updates with the central aggregation server. The central aggregation server received model updates from all collaborators, combined them (by averaging model parameters) and sent the consensus model back to each collaborator to continue their local training. Each such iteration is called a “*federated round*”. After not observing any meaningful changes since round 42, we stopped the training after a total of 73 federated rounds. Additionally, we performed all operations on the aggregator on secure hardware (by leveraging trusted execution environments⁷⁷), in order to increase the trust by all parties in the confidentiality of the model

updates being computed and shared, as well as to increase the confidence in the integrity of the computations being performed⁷⁸.

The federated training was initialized using a “*public initial model*” trained on 231 cases from 16 sites. This was done as opposed to a random initialization point to facilitate faster convergence of the model performance^{79,80}. After the training process was complete, the “*final consensus model*” was obtained after model selection from all the global consensus models obtained for each federated round. Thus, the final consensus model was developed on 6,314 cases from 71 sites. To quantitatively evaluate the performance of the trained models, 20% of the total cases contributed by each participating site were excluded from the model training process and were used as “*local validation data*”. To further evaluate the generalizability of the models in unseen data, 6 sites were not involved in any of the training stages to represent an unseen “out-of-sample” data population of 590 cases. To facilitate further evaluation without burdening the collaborating sites, a subset ($n = 332$) of these cases was aggregated to serve as a “*centralized out-of-sample*” dataset. Model performance was quantitatively evaluated here using the Dice Similarity Coefficient (*DSC*), which assesses the spatial agreement between the model’s prediction and the reference standard for each of the 3 tumor sub-compartments (ET, TC, WT).

Model Run-time in Clinical Environments

Clinical environments typically have constrained computational resources, such as the availability of specialized hardware (e.g., DL acceleration cards) and increased memory, which affect the run-time performance of DL inference workloads. Thus, taking into consideration the potential deployment of the final consensus model in such low-resource settings, we decided to proceed with a single 3D-ResUNet, rather than an ensemble of multiple models. This decision ensured a reduced computational burden, when compared with running multiple models, which is typically done in academic research projects^{54–57}.

To further facilitate use in low-resource environments, we plan to publicly release run-time optimized⁸¹ version of the final consensus model. For this model, graph level optimizations (i.e., operators fusion) were initially applied, followed by optimizations for low precision inference, i.e., converting the floating point single precision model to a fixed precision 8-bit integer model (a process known as “quantization”⁸²). In particular, we used accuracy-aware quantization⁸³, where model layers were iteratively scaled to a lower precision format. These optimizations yielded several run-time performance benefits, such as lower inference latency (a platform-dependent $4.48\times$ average speedup and $2.29\times$ reduced memory requirement when compared with the original consensus model), and higher throughput (equal to the $4.48\times$ speedup improvement since the batch size used is equal to 1), while the trade-off was an insignificant ($p_{Average} < 7 \times 10^{-5}$) drop in the average *DSC*.

Code availability

Motivated by findability, accessibility, interoperability, and reusability (FAIR) criteria in scientific research⁸⁴, all the code used to design the Federated Tumor Segmentation (FeTS) platform for this study is available at <https://github.com/FETS-AI/Front-End>. The functionality related to preprocessing (i.e., DICOM to NIfTI conversion, population-based harmonized preprocessing, co-registration) and manual refinements of annotation is derived from the open-source

Cancer Imaging Phenomics Toolkit (CaPTk, <https://github.com/CBICA/CaPTk>)⁸⁵⁻⁸⁷. The co-registration is performed using the Greedy framework⁸⁸, available via CaPTk⁸⁵⁻⁸⁷, ITK-SNAP⁸⁹, and the FeTS tool. The brain extraction⁹⁰ is done using the BrainMaGe method⁹¹, and is available in <https://github.com/CBICA/BrainMaGe> and via the Generally Nuanced Deep Learning Framework (GaNDLF)⁹² at <https://github.com/CBICA/GaNDLF>. To generate automated annotations, DeepMedic’s⁹³ integration with CaPTk was used, and we used the model weights and inference mechanism provided by the other algorithm developers (DeepScan⁹⁴ and nnU-Net⁷⁰ (<https://github.com/MIC-DKFZ/nnunet>)). DeepMedic’s original implementation is available in <https://github.com/deepmedic/deepmedic>, whereas the one we used in this study can be found at <https://github.com/CBICA/deepmedic>. The fusion of the labels was done using the Label Fusion tool⁹⁵ available at <https://github.com/FETS-AI/LabelFusion>. The data loading pipeline and network architecture was developed using the GaNDLF framework⁹² by using PyTorch⁹⁶. The data augmentation was done via GaNDLF by leveraging TorchIO⁹⁷. The FL backend developed for this project has been open-sourced as a separate software library, to encourage further research on FL⁹⁸ and is available at <https://github.com/intel/openfl>. The optimization of the consensus model inference workload was performed via OpenVINO⁹⁹ (<https://github.com/openvinotoolkit/openvino/tree/2021.4.1>), which is an open-source toolkit enabling acceleration of neural network models through various optimization techniques. The optimizations were evaluated on an Intel Core® i7-1185G7E CPU @ 2.80GHz with 2 × 8 GB DDR4 3200MHz memory on Ubuntu 18.04.6 OS and Linux kernel version 5.9.0-050900-generic.

Results

At the time of initialization of the federation, the public initial model was evaluated against the local validation data of all sites, resulting in an average (across all cases of all sites) DSC per sub-compartment, of: $DSC_{ET} = 0.63$, $DSC_{TC} = 0.62$, $DSC_{WT} = 0.75$. To summarize the model performance with a single collective score, we then calculate the average DSC (across all 3 tumor sub-compartments per case, and then across all cases of all sites) as equal to 0.66.

Following model training across all sites, the final consensus model garnered significant performance improvements against the collaborators’ local validation data of 27% ($p_{ET} < 1 \times 10^{-36}$), 33% ($p_{TC} < 1 \times 10^{-59}$), and 16% ($p_{WT} < 1 \times 10^{-21}$), for ET, TC, and WT, respectively (Fig. 1.c).

To further evaluate the potential generalizability improvements of the final consensus model on unseen data, we compared it with the public initial model against the complete out-of-sample data, and noted significant performance improvements of 15% ($p_{ET} < 1 \times 10^{-5}$), 27% ($p_{TC} < 1 \times 10^{-16}$), and 16% ($p_{WT} < 1 \times 10^{-7}$), for ET, TC, and WT, respectively (Fig. 1.d).

Notably, the only difference between the public initial model and the final consensus model, was that the latter gained knowledge during training from increased datasets contributed by the complete set of collaborators. The conclusion of these findings reinforces the importance of using large and diverse data for generalizable models to ultimately drive patient care.

Discussion

In this study, we have described the largest real-world FL effort to-date utilizing data of 6,314 glioblastoma patients from 71 geographically unique sites spread across 6 continents, to develop an accurate and generalizable ML model for detecting glioblastoma sub-compartment boundaries. Notably, this extensive global footprint of the collaborating sites in this study, also yield the largest dataset ever reported in the literature assessing this rare disease. It is the use of FL that successfully enabled *i)* access to such an unprecedented dataset of the most common and fatal adult brain tumor, and *ii)* meaningful ML training to ensure generalizability of models across out-of-sample data. Since glioblastoma boundary detection is critical for treatment planning and the requisite first step for further quantitative analyses, the models generated during this study have the potential to make far-reaching clinical impact.

The large and diverse data that FL enabled, led to the final consensus model garnering significant performance improvements over the public initial model against both the collaborators’ local validation data and the complete out-of-sample data. The improved result is a clear indication of the benefit that can be afforded through access to more data. In comparison with the limited existing real-world FL studies^{30,51}, our use case is larger in scale and substantially more complex, since it 1) addresses a multi-parametric multi-class problem, with reference standards that require expert collaborating clinicians to follow an involved manual annotation protocol, rather than simply recording a categorical entry from medical records, and 2) requires the data to be preprocessed in a harmonized manner to account for differences in MRI acquisition.

We have demonstrated the utility of an FL approach to develop an accurate and generalizable ML model for detecting glioblastoma sub-compartment boundaries, a finding which is of particular relevance for neurosurgical and radiotherapy planning in patients with this disease. This study is meant to be used as a blueprint for future FL studies that result in clinically deployable ML models. Building on this study, a continuous FL consortium would enable downstream quantitative analyses with implications for both routine practice and clinical trials, and most importantly, increase access to high-quality precision care worldwide. Furthermore, the lessons learned from this study with such a global footprint are invaluable and can be applied to a broad array of clinical scenarios with the potential for great impact to rare diseases and underrepresented populations.

Acknowledgments

Research and main methodological developments reported in this publication were partly supported by the National Institutes of Health (NIH) under award numbers NIH/NCI:U01CA242871 (S.Bakas), NIH/NINDS:R01NS042645 (C.Davatzikos), NIH/NCI:U24CA189523 (C.Davatzikos), NIH/NCI:U24CA215109 (J.Saltz), NIH/NCI:U01CA248226 (P.Tiwari), NIH/NCI:P30CA51008 (Y.Gusev), NIH:R50CA211270 (M.Muzi), NIH/NCATS:UL1TR001433 (Y.Yuan), NIH/NIBIB:R21EB030209 (Y.Yuan), NIH/NCI:R37CA214955 (A.Rao), and NIH:R01CA233888 (A.L.Simpson). The authors would also like to acknowledge the following NIH funded awards for the multi-site clinical trial (NCT00884741, RTOG0825/ACRIN6686): U10CA21661, U10CA37422, U10CA180820, U10CA180794, U01CA176110, R01CA082500, CA079778, CA080098, CA180794, CA180820,

CA180822, CA180868. Research reported in this publication was also partly supported by the National Science Foundation, under award numbers 2040532 (S.Baek), and 2040462 (B.Landman). Research reported in this publication was also supported by i) a research grant from Varian Medical Systems (Palo Alto, CA USA) (Y.Yuan), ii) the Ministry of Health of the Czech Republic (Grant Nr. NU21-08-00359) (M.Keřkovský and M.Kozubek), iii) Deutsche Forschungsgemeinschaft (DFG, German Research Foundation) Project-ID 404521405, SFB 1389, Work Package C02, and Priority Programme 2177 “Radiomics: Next Generation of Biomedical Imaging” (KI 2410/1-1 — MA 6340/18-1) (P.Vollmuth), iv) DFG Project-ID B12, SFB 824 (B.Wiestler), v) the Helmholtz Association (funding number ZT-I-OO1 4) (K.Maier-Hein), vi) the Dutch Cancer Society (KWF project number EMCR 2015-7859) (S.R.van der Voort), vii) the Chilean National Agency for Research and Development (ANID-Basal FB0008 (AC3E) and FB210017 (CENIA)) (P.Guevara), viii) the Canada CIFAR AI Chairs Program (M.Vallières), ix) Leeds Hospital Charity (Ref: 9RO1/1403) (S.Currie), x) the Cancer Research UK funding for the Leeds Radiotherapy Research Centre of Excellence (RadNet) and the grant number C19942/A28832 (S.Currie), xi) Medical Research Council (MRC) Doctoral Training Programme in Precision Medicine (Award Reference No. 2096671) (J.Bernal), xii) The European Research Council (ERC) under the European Union’s Horizon 2020 research and innovation programme (Grant Agreement No. 757173) (B.Glocker), xiii) The UKRI London Medical Imaging & Artificial Intelligence Centre for Value Based Healthcare (K.Kamnitsas), xiv) Wellcome/Engineering and Physical Sciences Research Council (EPSRC) Center for Medical Engineering (WT 203148/Z/16/Z) (T.C.Booth), xv) American Cancer Society Research Scholar Grant RSG-16-005-01 (A.Rao), xvi) the Department of Defense (DOD) Peer Reviewed Cancer Research Program (PRCRP) W81XWH-18-1-0404, Dana Foundation David Mahoney Neuroimaging Program, the V Foundation Translational Research Award, Johnson & Johnson WiSTEM2D Award (P.Tiwari), xvii) RSNA Research & Education Foundation under grant number RR2011 (E.Calabrese), xviii) the National Research Fund of Luxembourg (FNR) (grant number: C20/BM/14646004/GLASS-LUX/Niclou) (S.P.Niclou), xix) EU Marie Curie FP7-PEOPLE-2012-ITN project TRANSACT (PITN-GA-2012-316679) and the Swiss National Science Foundation (project number 140958) (J.Slotboom), and xx) CNPq 303808/2018-7 and FAPESP 2014/12236-1 (A.Xavier Falcão). The content of this publication is solely the responsibility of the authors and does not represent the official views of the NIH, the NSF, the RSNA R&E Foundation, or any of the additional funding bodies.

Author Contributions

Study Conception: S.Pati, U.Baid, B.Edwards, M.Sheller, G.A.Reina, J.Martin, S.Bakas.

Development of software used in the study: S.Pati, B.Edwards, M.Sheller, S.Wang, G.A.Reina, P.Foley, A.Gruzdev, D.Karkada.

Data Acquisition: M.Bilello, S.Mohan, E.Calabrese, J.Rudie, J.Saini, R.Y.Huang, K.Chang, T.So, P.Heng, T.F.Cloughesy, C.Raymond, T.Oughourlian, A.Hagiwara, C.Wang, M.To, M.Keřkovský, T.Kopřivová, M.Dostál, V.Vybíhal, J.A.Maldjian, M.C.Pinho, D.Reddy, J.Holcomb, B.Wiestler, M.Metz, R.Jain, M.Lee, P.Tiwari, R.Verma, Y.Gusev, K.Bhuvaneshwar, C.Bencheqroun, A.Belouali, A.Abayazeed, A.Abbassy, S.Gamal, M.Qayati, M.Mekhaimar, M.Reyes, R.R.Colen, M.Ak, P.Vollmuth, G.Brugnara, F.Sahm, M.Bendszus,

W.Wick, A.Mahajan, C.Balaña Quintero, J.Capellades, J.Puig, Y.Choi, M.Muzi, H.F.Shaykh, A.Herrera-Trujillo, W.Escobar, A.Abello, P.LaMontagne, B.Landman, K.Ramadass, K.Xu, S.Chotai, L.B.Chambless, A.Mistry, R.C.Thompson, J.Bapuraj, N.Wang, S.R.van der Voort, F.Incekara, M.M.J.Wijnenga, R.Gahrman, J.W.Schouten, H.J.Dubbink, A.J.P.E.Vincent, M.J.van den Bent, H.I.Sair, C.K.Jones, A.Venkataraman, J.Garrett, M.Larson, B.Menze, T.Weiss, M.Weller, A.Bink, B.Pouymayou, Y.Yuan, S.Sharma, T.Tseng, B.C.A.Teixeira, F.Sprenger, S.P.Niclou, O.Keunen, L.V.M.Dixon, M.Williams, R.G.H.Beets-Tan, H.Franco-Maldonado, F.Loayza, J.Slotboom, P.Radojewski, R.Meier, R.Wiest, J.Trenkler, J.Pichler, G.Necker, S.Meckel, E.Torche, F.Vera, E.Lóópez, Y.Kim, H.Ismael, B.Allen, J.M.Buatti, J.Park, P.Zampakis, V.Panagiotopoulos, P.Tsiganos, E.Challiasos, D.M.Kardamakis, P.Prasanna, K.M.Mani, D.Payne, T.Kurc, L.Poisson, M.Vallièrès, D.Fortin, M.Lepage, F.Morón, J.Mandel, C.Badve, A.E.Sloan, J.S.Barnholtz-Sloan, K.Waite, G.Shukla, S.Liem, G.S.Alexandre, J.Lombardo, J.D.Palmer, A.E.Flanders, A.P.Dicker, G.Ogbole, M.Soneye, D.Oyekunle, O.Odafa-Oyibotha, B.Osobu, M.Shu'aibu, F.Dako, A.Dorcas, D.Murcia, R.Haas, J.Thompson, D.R.Ormond, S.Currie, K.Fatania, R.Frood, J.Mitchell, J.Farinhas, A.L.Simpson, J.J.Peoples, R.Hu, D.Cutler, F.Y.Moraes, A.Tran, M.Hamghalam, M.A.Boss, J.Gimpel, B.Bialecki, A.Chelliah.

Data Processing: C.Sako, S.Ghodasara, E.Calabrese, J.Rudie, M.Jadhav, U.Pandey, R.Y.Huang, M.Jiang, C.Chen, C.Raymond, S.Bhardwaj, C.Chong, M.Agzarian, M.Kozubek, F.Lux, J.Michálek, P.Matula, C.Bangalore Yogananda, D.Reddy, B.C.Wagner, I.Ezhov, M.Lee, Y.W.Lui, R.Verma, R.Bareja, I.Yadav, J.Chen, N.Kumar, K.Bhuvaneshwar, A.Sayah, C.Bencheqroun, K.Kolodziej, M.Hill, M.Reyes, L.Pei, M.Ak, A.Kotrotsou, P.Vollmuth, G.Brugnara, C.J.Preetha, M.Zenk, J.Puig, M.Muzi, H.F.Shaykh, A.Abello, J.Bernal, J.Gómez, P.LaMontagne, K.Ramadass, S.Chotai, N.Wang, M.Smits, S.R.van der Voort, A.Alafandi, F.Incekara, M.M.J.Wijnenga, G.Kapsas, R.Gahrman, A.J.P.E.Vincent, P.J.French, S.Klein, H.I.Sair, C.K.Jones, J.Garrett, H.Li, F.Kofler, Y.Yuan, S.Adabi, A.Xavier Falcão, S.B.Martins, D.Menotti, D.R.Lucio, O.Keunen, A.Hau, K.Kamnitsas, L.Dixon, S.Benson, E.Pelaez, H.Franco-Maldonado, F.Loayza, S.Quevedo, R.McKinley, J.Trenkler, A.Haunschmidt, C.Mendoza, E.Ríos, J.Choi, S.Baek, J.Yun, P.Zampakis, V.Panagiotopoulos, P.Tsiganos, E.I.Zacharaki, C.Kalogeropoulou, P.Prasanna, S.Shreshtra, T.Kurc, B.Luo, N.Wen, M.Vallièrès, D.Fortin, F.Morón, C.Badve, V.Vadmal, G.Shukla, G.Ogbole, D.Oyekunle, F.Dako, D.Murcia, E.Fu, S.Currie, R.Frood, M.A.Vogelbaum, J.Mitchell, J.Farinhas, J.J.Peoples, M.Hamghalam, D.Kattil Veetil, K.Schmidt, B.Bialecki, S.Marella, T.C.Booth, A.Chelliah, M.Modat, C.Dragos, H.Shuaib.

Data Analysis & Interpretation: S.Pati, U.Baid, B.Edwards, M.Sheller, S.Bakas.

Site PI/Senior member (of each collaborating group): C.Davatzikos, J.Villanueva-Meyer, M.Ingalhalikar, R.Y.Huang, Q.Dou, B.M.Ellingson, M.To, M.Kozubek, J.A.Maldjian, B.Wiestler, R.Jain, P.Tiwari, Y.Gusev, A.Abayazeed, R.R.Colen, P.Vollmuth, A.Mahajan, C.Balaña Quintero, S.Lee, M.Muzi, H.F.Shaykh, M.Trujillo, D.Marcus, B.Landman, A.Rao, M.Smits, H.I.Sair, R.Jeraj, B.Menze, Y.Yuan, A.Xavier Falcão, S.P.Niclou, B.Glocker, J.Teuwen, E.Pelaez, R.Wiest, S.Meckel, P.Guevara, S.Baek, H.Kim, D.M.Kardamakis, J.Saltz, L.Poisson, M.Vallièrès, F.Morón, A.E.Sloan, A.E.Flanders, G.Ogbole, D.R.Ormond, S.Currie, J.Farinhas, A.L.Simpson, C.Apgar, T.C.Booth.

Writing the Original Manuscript: S.Pati, U.Baid, B.Edwards, M.Sheller, S.Bakas.

Review, Edit, & Approval of the Final Manuscript: All authors.

Competing Interest Declaration

The Intel affiliated authors (B.Edwards, M.Sheller, S.Wang, G.A.Reina, P.Foley, A.Gruzdev, D.Karkada, P.Shah, J.Martin) would like to disclose the following (potential) competing interest as Intel employees. Intel may develop proprietary software that is related in reputation to the OpenFL open source project highlighted in this work. In addition, the work demonstrates feasibility of federated learning for brain tumor boundary detection models. Intel may benefit by selling products to support an increase in demand for this use case.

References

- [1] Hamed Akbari et al. “Pattern analysis of dynamic susceptibility contrast-enhanced MR imaging demonstrates peritumoral tissue heterogeneity”. In: *Radiology* 273.2 (2014), pp. 502–510.
- [2] Hamed Akbari et al. “Imaging surrogates of infiltration obtained via multiparametric imaging pattern analysis predict subsequent location of recurrence of glioblastoma”. In: *Neurosurgery* 78.4 (2016), pp. 572–580.
- [3] Spyridon Bakas et al. “In vivo detection of EGFRvIII in glioblastoma via perfusion magnetic resonance imaging signature consistent with deep peritumoral infiltration: the φ -index”. In: *Clinical Cancer Research* 23.16 (2017), pp. 4724–4734.
- [4] Hamed Akbari et al. “In vivo evaluation of EGFRvIII mutation in primary glioblastoma patients via complex multiparametric MRI signature”. In: *Neuro-oncology* 20.8 (2018), pp. 1068–1079.
- [5] Zev A Binder et al. “Epidermal growth factor receptor extracellular domain mutations in glioblastoma present opportunities for clinical imaging and therapeutic development”. In: *Cancer cell* 34.1 (2018), pp. 163–177.
- [6] Saima Rathore et al. “Deriving stable multi-parametric MRI radiomic signatures in the presence of inter-scanner variations: survival prediction of glioblastoma via imaging pattern analysis and machine learning techniques”. In: *Medical Imaging 2018: Computer-Aided Diagnosis*. Vol. 10575. International Society for Optics and Photonics. 2018, p. 1057509.
- [7] Spyridon Bakas et al. “NIMG-40. Non-invasive in vivo signature of idh1 mutational status in high grade glioma, from clinically-acquired multi-parametric magnetic resonance imaging, using multivariate machine learning”. In: *Neuro-Oncology* 20.suppl_6 (2018), pp. vi184–vi185.
- [8] Jared M Pisapia et al. “Use of fetal magnetic resonance image analysis and machine learning to predict the need for postnatal cerebrospinal fluid diversion in fetal ventriculomegaly”. In: *JAMA pediatrics* 172.2 (2018), pp. 128–135.
- [9] Christos Davatzikos et al. “Precision diagnostics based on machine learning-derived imaging signatures”. In: *Magnetic resonance imaging* 64 (2019), pp. 49–61.
- [10] Anahita Fathi Kazerooni et al. “Imaging signatures of glioblastoma molecular characteristics: a radiogenomics review”. In: *Journal of Magnetic Resonance Imaging* 52.1 (2020), pp. 54–69.

- [11] Spyridon Bakas et al. “Overall survival prediction in glioblastoma patients using structural magnetic resonance imaging (MRI): advanced radiomic features may compensate for lack of advanced MRI modalities”. In: *Journal of Medical Imaging* 7.3 (2020), p. 031505.
- [12] Hamed Akbari et al. “Histopathology-validated machine learning radiographic biomarker for noninvasive discrimination between true progression and pseudo-progression in glioblastoma”. In: *Cancer* 126.11 (2020), pp. 2625–2636.
- [13] Andreas Mang et al. “Integrated biophysical modeling and image analysis: application to neuro-oncology”. In: *Annual review of biomedical engineering* 22 (2020), pp. 309–341.
- [14] Bjoern Menze et al. “Analyzing magnetic resonance imaging data from glioma patients using deep learning”. In: *Computerized medical imaging and graphics* 88 (2021), p. 101828.
- [15] Gustav Mårtensson et al. “The reliability of a deep learning model in clinical out-of-distribution MRI data: a multicohort study”. In: *Medical Image Analysis* 66 (2020), p. 101714.
- [16] John R Zech et al. “Variable generalization performance of a deep learning model to detect pneumonia in chest radiographs: a cross-sectional study”. In: *PLoS medicine* 15.11 (2018), e1002683.
- [17] Ziad Obermeyer and Ezekiel J Emanuel. “Predicting the future—big data, machine learning, and clinical medicine”. In: *The New England journal of medicine* 375.13 (2016), p. 1216.
- [18] Gary Marcus. “Deep learning: A critical appraisal”. In: *arXiv preprint arXiv:1801.00631* (2018).
- [19] Charu C Aggarwal et al. “Neural networks and deep learning”. In: *Springer* 10 (2018), pp. 978–3.
- [20] Paul M Thompson et al. “The ENIGMA Consortium: large-scale collaborative analyses of neuroimaging and genetic data”. In: *Brain imaging and behavior* 8.2 (2014), pp. 153–182.
- [21] The GLASS Consortium. “Glioma through the looking GLASS: molecular evolution of diffuse gliomas and the Glioma Longitudinal Analysis Consortium”. In: *Neuro-Oncology* 20.7 (Feb. 2018), pp. 873–884. ISSN: 1522-8517.
- [22] Christos Davatzikos et al. “AI-based prognostic imaging biomarkers for precision neuro-oncology: the ReSPOND consortium”. In: *Neuro-oncology* 22.6 (2020), pp. 886–888.
- [23] Spyridon Bakas et al. “iGLASS: imaging integration into the Glioma Longitudinal Analysis Consortium”. In: *Neuro-oncology* 22.10 (2020), pp. 1545–1546.
- [24] Nicola Rieke et al. “The future of digital health with federated learning”. In: *NPJ digital medicine* 3.1 (2020), pp. 1–7.
- [25] Micah J Sheller et al. “Federated learning in medicine: facilitating multi-institutional collaborations without sharing patient data”. In: *Scientific reports* 10.1 (2020), pp. 1–12.
- [26] George J Annas et al. “HIPAA regulations-a new era of medical-record privacy?” In: *New England Journal of Medicine* 348.15 (2003), pp. 1486–1490.
- [27] Paul Voigt and Axel Von dem Bussche. “The eu general data protection regulation (gdpr)”. In: *A Practical Guide, 1st Ed., Cham: Springer International Publishing* 10 (2017), p. 3152676.

- [28] Brendan McMahan et al. “Communication-efficient learning of deep networks from decentralized data”. In: *Artificial intelligence and statistics*. PMLR. 2017, pp. 1273–1282.
- [29] Micah J Sheller et al. “Multi-institutional deep learning modeling without sharing patient data: A feasibility study on brain tumor segmentation”. In: *International MICCAI Brainlesion Workshop*. Springer. 2018, pp. 92–104.
- [30] Ittai Dayan et al. “Federated learning for predicting clinical outcomes in patients with COVID-19”. In: *Nature medicine* 27.10 (2021), pp. 1735–1743.
- [31] Ken Chang et al. “Distributed deep learning networks among institutions for medical imaging”. In: *Journal of the American Medical Informatics Association* 25.8 (2018), pp. 945–954.
- [32] Adrian Nilsson et al. “A performance evaluation of federated learning algorithms”. In: *Proceedings of the Second Workshop on Distributed Infrastructures for Deep Learning*. 2018, pp. 1–8.
- [33] Karthik V Sarma et al. “Federated learning improves site performance in multicenter deep learning without data sharing”. In: *Journal of the American Medical Informatics Association* 28.6 (2021), pp. 1259–1264.
- [34] Chen Shen et al. “Multi-task Federated Learning for Heterogeneous Pancreas Segmentation”. In: *Clinical Image-Based Procedures, Distributed and Collaborative Learning, Artificial Intelligence for Combating COVID-19 and Secure and Privacy-Preserving Machine Learning*. Springer, 2021, pp. 101–110.
- [35] Dong Yang et al. “Federated semi-supervised learning for COVID region segmentation in chest CT using multi-national data from China, Italy, Japan”. In: *Medical image analysis* 70 (2021), p. 101992.
- [36] Jeffrey De Fauw et al. “Clinically applicable deep learning for diagnosis and referral in retinal disease”. In: *Nature medicine* 24.9 (2018), pp. 1342–1350.
- [37] Awni Y Hannun et al. “Cardiologist-level arrhythmia detection and classification in ambulatory electrocardiograms using a deep neural network”. In: *Nature medicine* 25.1 (2019), pp. 65–69.
- [38] Robert C Griggs et al. “Clinical research for rare disease: opportunities, challenges, and solutions”. In: *Molecular genetics and metabolism* 96.1 (2009), pp. 20–26.
- [39] Gaurav Shukla et al. “Advanced magnetic resonance imaging in glioblastoma: a review”. In: *Chin Clin Oncol* 6.4 (2017), p. 40.
- [40] Cameron W Brennan et al. “The somatic genomic landscape of glioblastoma”. In: *Cell* 155.2 (2013), pp. 462–477.
- [41] Roel GW Verhaak et al. “Integrated genomic analysis identifies clinically relevant subtypes of glioblastoma characterized by abnormalities in PDGFRA, IDH1, EGFR, and NF1”. In: *Cancer cell* 17.1 (2010), pp. 98–110.
- [42] Andrea Sottoriva et al. “Intratumor heterogeneity in human glioblastoma reflects cancer evolutionary dynamics”. In: *Proceedings of the National Academy of Sciences* 110.10 (2013), pp. 4009–4014.
- [43] Quinn T Ostrom et al. “CBTRUS statistical report: primary brain and other central nervous system tumors diagnosed in the United States in 2012–2016”. In: *Neuro-oncology* 21.Supplement_5 (2019), pp. v1–v100.
- [44] David N Louis et al. “The 2021 WHO classification of tumors of the central nervous system: a summary”. In: *Neuro-oncology* 23.8 (2021), pp. 1231–1251.

- [45] W Han et al. “Deep transfer learning and radiomics feature prediction of survival of patients with high-grade gliomas”. In: *American Journal of Neuroradiology* 41.1 (2020), pp. 40–48.
- [46] Spyridon Bakas et al. “GLISTRboost: combining multimodal MRI segmentation, registration, and biophysical tumor growth modeling with gradient boosting machines for glioma segmentation”. In: *BrainLes 2015*. Springer. 2015, pp. 144–155.
- [47] Spyridon Bakas et al. “Segmentation of gliomas in multimodal magnetic resonance imaging volumes based on a hybrid generative-discriminative framework”. In: *Proceeding of the Multimodal Brain Tumor Image Segmentation Challenge* (2015), pp. 5–12.
- [48] Ke Zeng et al. “Segmentation of gliomas in pre-operative and post-operative multimodal magnetic resonance imaging volumes based on a hybrid generative-discriminative framework”. In: *International Workshop on Brainlesion: Glioma, Multiple Sclerosis, Stroke and Traumatic Brain Injuries*. Springer. 2016, pp. 184–194.
- [49] Jeffrey D Rudie et al. “Multi-disease segmentation of gliomas and white matter hyperintensities in the BraTS data using a 3D convolutional neural network”. In: *Frontiers in Computational Neuroscience* 13 (2019), p. 84.
- [50] Linmin Pei et al. “Longitudinal brain tumor segmentation prediction in MRI using feature and label fusion”. In: *Biomedical signal processing and control* 55 (2020), p. 101648.
- [51] Holger R Roth et al. “Federated learning for breast density classification: A real-world implementation”. In: *Domain Adaptation and Representation Transfer, and Distributed and Collaborative Learning*. Springer, 2020, pp. 181–191.
- [52] Kaisorn L Chaichana et al. “Multi-institutional validation of a preoperative scoring system which predicts survival for patients with glioblastoma”. In: *Journal of Clinical Neuroscience* 20.10 (2013), pp. 1422–1426.
- [53] Anahita Fathi Kazerooni et al. “Cancer imaging phenomics via CaPTk: multi-institutional prediction of progression-free survival and pattern of recurrence in glioblastoma”. In: *JCO clinical cancer informatics* 4 (2020), pp. 234–244.
- [54] Bjoern H Menze et al. “The multimodal brain tumor image segmentation benchmark (BRATS)”. In: *IEEE transactions on medical imaging* 34.10 (2014), pp. 1993–2004.
- [55] Spyridon Bakas et al. “Advancing the cancer genome atlas glioma MRI collections with expert segmentation labels and radiomic features”. In: *Scientific data* 4.1 (2017), pp. 1–13.
- [56] Spyridon Bakas et al. “Identifying the best machine learning algorithms for brain tumor segmentation, progression assessment, and overall survival prediction in the BRATS challenge”. In: *arXiv preprint arXiv:1811.02629* (2018).
- [57] Ujjwal Baid et al. “The rsna-asnr-miccai brats 2021 benchmark on brain tumor segmentation and radiogenomic classification”. In: *arXiv preprint arXiv:2107.02314* (2021).
- [58] Mark R Gilbert et al. *RTOG 0825: Phase III double-blind placebo-controlled trial evaluating bevacizumab (Bev) in patients (Pts) with newly diagnosed glioblastoma (GBM)*. 2013.
- [59] Mark R Gilbert et al. “A randomized trial of bevacizumab for newly diagnosed glioblastoma”. In: *New England Journal of Medicine* 370.8 (2014), pp. 699–708.
- [60] Jerrold L Boxerman et al. “Prognostic value of contrast enhancement and FLAIR for survival in newly diagnosed glioblastoma treated with and without bevacizumab: results from ACRIN 6686”. In: *Neuro-oncology* 20.10 (2018), pp. 1400–1410.

- [61] Kathleen M Schmainda et al. “Value of dynamic contrast perfusion MRI to predict early response to bevacizumab in newly diagnosed glioblastoma: results from ACRIN 6686 multicenter trial”. In: *Neuro-oncology* 23.2 (2021), pp. 314–323.
- [62] Olaf Ronneberger, Philipp Fischer, and Thomas Brox. “U-net: Convolutional networks for biomedical image segmentation”. In: *International Conference on Medical image computing and computer-assisted intervention*. Springer. 2015, pp. 234–241.
- [63] Özgün Çiçek et al. “3D U-Net: learning dense volumetric segmentation from sparse annotation”. In: *International conference on medical image computing and computer-assisted intervention*. Springer. 2016, pp. 424–432.
- [64] Kaiming He et al. “Deep residual learning for image recognition”. In: *Proceedings of the IEEE conference on computer vision and pattern recognition*. 2016, pp. 770–778.
- [65] Michal Drozdal et al. “The importance of skip connections in biomedical image segmentation”. In: *Deep Learning and Data Labeling for Medical Applications*. Springer, 2016, pp. 179–187.
- [66] Megh Bhalerao and Siddhesh Thakur. “Brain tumor segmentation based on 3D residual U-Net”. In: *International MICCAI Brainlesion Workshop*. Springer. 2019, pp. 218–225.
- [67] Diederik P Kingma and Jimmy Ba. “Adam: A method for stochastic optimization”. In: *arXiv preprint arXiv:1412.6980* (2014).
- [68] Carole H Sudre et al. “Generalised dice overlap as a deep learning loss function for highly unbalanced segmentations”. In: *Deep learning in medical image analysis and multimodal learning for clinical decision support*. Springer, 2017, pp. 240–248.
- [69] Alex P Zijdenbos et al. “Morphometric analysis of white matter lesions in MR images: method and validation”. In: *IEEE transactions on medical imaging* 13.4 (1994), pp. 716–724.
- [70] Fabian Isensee et al. “nnU-Net: a self-configuring method for deep learning-based biomedical image segmentation”. In: *Nature Methods* 18.2 (2021), pp. 203–211.
- [71] Liangjun Chen et al. “Efficient and robust deep learning with correntropy-induced loss function”. In: *Neural Computing and Applications* 27.4 (2016), pp. 1019–1031.
- [72] Seyed Sadegh Mohseni Salehi, Deniz Erdogmus, and Ali Gholipour. “Tversky loss function for image segmentation using 3D fully convolutional deep networks”. In: *International workshop on machine learning in medical imaging*. Springer. 2017, pp. 379–387.
- [73] Francesco Caliva et al. “Distance map loss penalty term for semantic segmentation”. In: *arXiv preprint arXiv:1908.03679* (2019).
- [74] Reuben R Shamir et al. “Continuous dice coefficient: a method for evaluating probabilistic segmentations”. In: *arXiv preprint arXiv:1906.11031* (2019).
- [75] Roger A Horn. “The hadamard product”. In: *Proc. Symp. Appl. Math.* Vol. 40. 1990, pp. 87–169.
- [76] Ian Barrodale. “L1 approximation and the analysis of data”. In: *Journal of the Royal Statistical Society: Series C (Applied Statistics)* 17.1 (1968), pp. 51–57.
- [77] Georgios A Kaissis et al. “Secure, privacy-preserving and federated machine learning in medical imaging”. In: *Nature Machine Intelligence* 2.6 (2020), pp. 305–311.
- [78] Jan-Erik Ekberg, Kari Kostianen, and N Asokan. “The untapped potential of trusted execution environments on mobile devices”. In: *IEEE Security & Privacy* 12.4 (2014), pp. 29–37.

- [79] Maithra Raghu et al. “Transfusion: Understanding transfer learning for medical imaging”. In: *Advances in neural information processing systems* 32 (2019).
- [80] Julio Cristian Young and Alethea Suryadibrata. “Applicability of various pre-trained deep convolutional neural networks for pneumonia classification based on X-Ray Images”. In: *International Journal of Advanced Trends in Computer Science and Engineering* 9.3 (2020).
- [81] Andres Rodriguez et al. “Lower numerical precision deep learning inference and training”. In: *Intel White Paper* 3 (2018), pp. 1–19.
- [82] Darryl Lin, Sachin Talathi, and Sreekanth Annapureddy. “Fixed point quantization of deep convolutional networks”. In: *International conference on machine learning*. PMLR. 2016, pp. 2849–2858.
- [83] Shervin Vakili, JM Pierre Langlois, and Guy Bois. “Enhanced precision analysis for accuracy-aware bit-width optimization using affine arithmetic”. In: *IEEE Transactions on Computer-Aided Design of Integrated Circuits and Systems* 32.12 (2013), pp. 1853–1865.
- [84] Mark D Wilkinson et al. “The FAIR Guiding Principles for scientific data management and stewardship”. In: *Scientific data* 3.1 (2016), pp. 1–9.
- [85] Christos Davatzikos et al. “Cancer imaging phenomics toolkit: quantitative imaging analytics for precision diagnostics and predictive modeling of clinical outcome”. In: *Journal of medical imaging* 5.1 (2018), p. 011018.
- [86] Saima Rathore et al. “Brain cancer imaging phenomics toolkit (brain-CaPTk): an interactive platform for quantitative analysis of glioblastoma”. In: *International MICCAI Brainlesion Workshop*. Springer. 2017, pp. 133–145.
- [87] Sarthak Pati et al. “The cancer imaging phenomics toolkit (captk): Technical overview”. In: *International MICCAI Brainlesion Workshop*. Springer. 2019, pp. 380–394.
- [88] Paul A Yushkevich et al. “Fast automatic segmentation of hippocampal subfields and medial temporal lobe subregions in 3 Tesla and 7 Tesla T2-weighted MRI”. In: *Alzheimer’s & Dementia: The Journal of the Alzheimer’s Association* 12.7 (2016), P126–P127.
- [89] Paul A. Yushkevich et al. “User-Guided 3D Active Contour Segmentation of Anatomical Structures: Significantly Improved Efficiency and Reliability”. In: *Neuroimage* 31.3 (2006), pp. 1116–1128.
- [90] Xu Han et al. “Brain extraction from normal and pathological images: A joint PCA/image-reconstruction approach”. In: *NeuroImage* 176 (2018), pp. 431–445.
- [91] Siddhesh Thakur et al. “Brain extraction on MRI scans in presence of diffuse glioma: Multi-institutional performance evaluation of deep learning methods and robust modality-agnostic training”. In: *NeuroImage* 220 (2020), p. 117081.
- [92] Sarthak Pati et al. “Gandlf: A generally nuanced deep learning framework for scalable end-to-end clinical workflows in medical imaging”. In: *arXiv preprint arXiv:2103.01006* (2021).
- [93] Konstantinos Kamnitsas et al. “Efficient multi-scale 3D CNN with fully connected CRF for accurate brain lesion segmentation”. In: *Medical image analysis* 36 (2017), pp. 61–78.
- [94] Richard McKinley, Raphael Meier, and Roland Wiest. “Ensembles of densely-connected CNNs with label-uncertainty for brain tumor segmentation”. In: *International MICCAI Brainlesion Workshop*. Springer. 2018, pp. 456–465.

- [95] Sarthak Pati and Spyridon Bakas. *LabelFusion: Medical Image label fusion of segmentations*. Version 1.0.10. Mar. 2021.
- [96] Adam Paszke et al. “Pytorch: An imperative style, high-performance deep learning library”. In: *Advances in neural information processing systems*. 2019, pp. 8026–8037.
- [97] Fernando Pérez-García, Rachel Sparks, and Sébastien Ourselin. “TorchIO: a Python library for efficient loading, preprocessing, augmentation and patch-based sampling of medical images in deep learning”. In: *Computer Methods and Programs in Biomedicine* (2021), p. 106236. ISSN: 0169-2607.
- [98] G Anthony Reina et al. “OpenFL: An open-source framework for Federated Learning”. In: *arXiv preprint arXiv:2105.06413* (2021).
- [99] Yury Gorbachev et al. “OpenVINO deep learning workbench: Comprehensive analysis and tuning of neural networks inference”. In: *Proceedings of the IEEE/CVF International Conference on Computer Vision Workshops*. 2019, pp. 783–787.